Optics Communications 284 (2011) 4465–4469

Contents lists available at ScienceDirect

Optics Communications

journal homepage: www.elsevier.com/locate/optcom

Optical clock recovery with dual-wavelength output from degraded RZ and NRZ signals

Shilong Pan [a,b,*], Caiyun Lou [a], Xiaofan Zhao [a], De Ben [b]

[a] TNList and State Key Laboratory on Integrated Optoelectronics, Department of Electronic Engineering, Tsinghua University, Beijing 100084, China
[b] College of Electronic and Information Engineering, Nanjing University of Aeronautics and Astronautics, Nanjing, Jiangsu 210016, China

ARTICLE INFO

Article history:
Received 29 September 2010
Received in revised form 31 March 2011
Accepted 12 May 2011
Available online 30 May 2011

Keywords:
Optical signal processing
Clock recovery
Mode-locked laser
Optoelectronic oscillator

ABSTRACT

A novel scheme to implement clock recovery from degraded signals is proposed and demonstrated based on an optoelectronic oscillator and a dual-wavelength mode-locked fiber ring laser with distributed dispersion cavity. The scheme can obtain wavelength-tunable optical clocks at two wavelengths, which is highly desirable for composite optical logic gates, cascaded optical signal processing modules or optical signal processing modules that need synchronized pulses at multiple wavelengths. In addition, the scheme can operate in both RZ and NRZ systems. The feasibility of the method is demonstrated by an experiment, in which dual-wavelength 10-GHz optical clock with a timing jitter less than 170 fs is obtained from 10-Gb/s degraded RZ and NRZ signals. The optical clocks can be tuned from 1530 to 1565 nm.

1. Introduction

Optical clock recovery from data signals is essential for optical signal processing applications in digital communication systems, such as 3R (reamplifation, retiming, and reshaping) regeneration, format conversion, optical logic gates, and signal demultiplexing [1]. Previously, optical clock recovery from a high-speed digital signal was reported using injection-locked mode-locked lasers [2–4], self-pulsing lasers [5], phase-locked loops [6] or optoelectronic oscillators (OEOs) [7–9]. These techniques, however, can only achieve optical clock at a single wavelength. For composite optical logic gates or cascaded optical signal processing modules, optical clocks at multiple wavelengths are required to avoid interference between different units. Multiwavelength optical clocks are also essential for OTDM-to-WDM conversion [10], optical serial-to-parallel conversion [11], and optical analog-to-digital conversion [12]. Since the optical signal for processing may be distorted by long-distance fiber transmission, it would be highly desirable that the clock recovery module has the capability to perform clock extraction from a degraded signal. In addition, the previous schemes can only operate in either return-to-zero (RZ) or non-return-to-zero (NRZ) systems. Since the two modulation formats may be selectively used in the future optical networks, it would be interesting to develop a scheme that can operate in both RZ and NRZ systems.

In this paper, we propose and demonstrate a novel scheme to realize optical clock recovery, which consists of an OEO and a dual-wavelength mode-locked fiber ring laser (MLFRL) with a distributed dispersion cavity. The combination of the two parts enables the extraction of high-quality optical clocks at multiple wavelengths from degraded RZ and NRZ signals. The wavelengths of the recovered optical clock can be tuned in the operating wavelength range of an erbium-doped fiber amplifier (EDFA). An experiment is performed, dual-wavelength 10-GHz optical clocks with timing jitter less than 170 fs are successfully recovered from 10-Gb/s degraded RZ and NRZ signals.

2. Principle

Fig. 1 shows the schematic of the proposed optical clock recovery system, which is composed of an OEO and a dual-wavelength MLFRL with a distributed dispersion cavity.

The OEO is constructed from a Mach–Zehnder modulator (MZM), a photodetector (PD), an electrical amplifier (EA), a narrow-bandwidth electrical bandpass filter (EBPF) and an electrical phase shifter (PS). An optical bandpass filter (OBPF1) is inserted to make sure that only the input data can enter into the OEO loop. The net gain of the loop is controlled to be greater than unity. If a continuous-wave (CW) lightwave is introduced into the modulator, the OEO will operate at free-running mode [8]. The center frequency ($f = m/\tau$, where m is an integer and τ is the loop delay), is determined by the center frequency of the EBPF and the loop delay. If an incoming data signal contains a clock with a frequency near the oscillating frequency is injected, the OEO will be injection locked by the clock component in the data signal. Clock recovery is then performed.

The dual-wavelength MLFRL shares the MZM with the OEO, which acts as the optical mode-locking element. Due to the polarization

* Corresponding author. Tel.: +86 2584896030; fax: +86 2584892848.
E-mail address: pans@ieee.org (S. Pan).

0030-4018/$ – see front matter © 2011 Elsevier B.V. All rights reserved.
doi:10.1016/j.optcom.2011.05.029

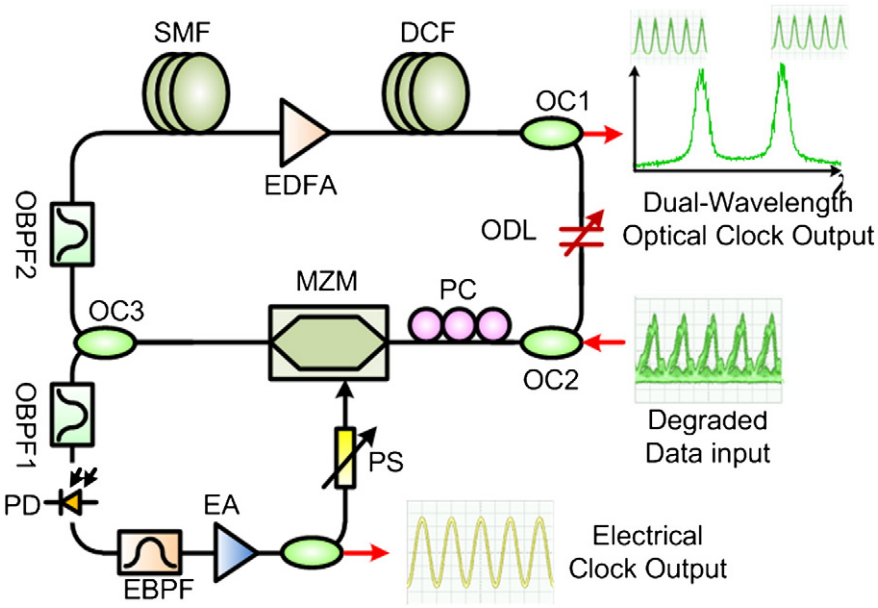

Fig. 1. Schematic of the proposed optical clock recovery system. SMF: single-mode fiber; EDFA: erbium-doped fiber amplifier; DCF: dispersion-compensating fiber; OC: optical coupler; ODL: optical delay line; PC: polarization controller; MZM: Mach–Zehnder modulator; OBPF: optical bandpass filter; PS: phase shifter; EA: electrical amplifier; EBPF: electrical bandpass filter; PD: photodetector.

dependence of the MZM, a polarization controller (PC) is incorporated at its input for performance optimization. The gain of the MLFRL is provided by an EDFA. The EDFA includes two polarization-independent isolators, which ensures the unidirectional operation. A tunable OBPF (OBPF2) is inserted to restrict the work bandwidth of the laser, which is also used to remove the data signal from the MLFRL. A tunable optical delay line (ODL) is used to adjust the cavity length. Intracavity group velocity dispersion was introduced by two dispersive elements, i.e. a length of single-mode fiber (SMF) and a length of dispersion-compensating fiber (DCF), placed before and after the EDFA, respectively.

The principle of the dual-wavelength clock recovery is described as follows. When a RZ signal with a data rate near the oscillating frequency of the OEO is injected into the scheme, the OEO would be injection locked since the RZ signal contains a strong clock component. A high spectral purity electrical clock will be obtained, which is then fed back into the RF port of the MZM. Since the MZM is also the mode-locking element in the cavity of the MLFRL, the MLFRL would be mode-locked and synchronized to the electrical clock. Due to the dispersive cavity, simultaneously multi-wavelength mode-locking is allowed [13,14]. The bandwidth of OBPF2 is selected to allow that only two wavelengths can oscillate. The gain competition between the two wavelengths, introduced by the strong homogeneous line broadening and cross-gain saturation in the erbium-doped fiber (EDF), is partly suppressed by the distributed dispersion cavity. With the distributed dispersion cavity, pulses at different wavelengths are separated in the time domain by the dispersive element before the EDF. Although the fluorescence lifetime of erbium ions in a glass host is very long, the gain recovery time of an EDFA can be controlled to be the order of nanoseconds by using short optical pulses to rapidly saturate the amplifier gain [15], which is always the case when the EDFA is applied as the gain provider in a MLFRL. Therefore, the short optical pulses split by tens of picoseconds would get some separated gain in the EDF, and the gain competition between the two wavelengths is reduced. Then, the split pulses are recombined or mismatched with exactly integral bit periods by the second dispersive element placed after the EDF. This method, although not eliminate the cross-gain saturation in the EDF, is sufficient to guarantee stable dual-wavelength lasing in the MLFRL, as experimentally validated in [16]. Optical clocks at two wavelengths are thus generated. Due to the dispersive cavity, smoothly wavelength tuning can be achieved by changing the cavity length [13,14], which is implemented by adjusting the tunable optical delay line.

Since the OEO is an oscillator with a very high Q value, the clock extraction can be performed as long as the injection signal has a distinct clock component [8]. Therefore, the clock recovery can be performed on a degraded signal if the distinct clock component is not eliminated.

It is well known that the electrical spectrum of an ideal NRZ signal contains no clock components. In the real case, however, a weak clock component always exists due to the imperfect multiplexing in the electrical domain to generate the high data rate electrical NRZ signal. Once the clock component is present, it would be captured and amplified by the OEO. The amplified clock component is then fed back into the MZM and modulates the later injected NRZ signal. With the modulation, the clock component in the injection signal is greatly enhanced. This positive feedback finally lead to an oscillation [7,17]. Thus, clock recovery from the NRZ signal can also be performed. Since the major sources for signal degradation, such as chromatic dispersion and nonlinear effects, would enhance the clock component in the NRZ signal [18,19], the scheme can extract clocks from degraded NRZ signal.

3. Results and discussions

An experiment is carried out based on the setup shown in Fig. 1. The parameters of the devices used in the experiment are as follows. The $LiNbO_3$ MZM has a bandwidth of 12.5 GHz and a half-wave voltage of 6 V. The PD has a bandwidth of 10 GHz. The bandwidth of the EBPF is 15 MHz centered at 9.953 GHz. The 3-dB bandwidths of OBPF1 and OBPF2 are 0.6 and 2.8 nm, respectively. The output saturation power of the EDFA is 16.6 dBm. The dispersion of the SMF and DCF is 33 and −96.2 ps/nm at 1550 nm, respectively. The coupling ratios of the three couplers, i.e. OC1, OC2 and OC3, are 9:1, 5:5 and 7:3. The waveforms are observed by a high-speed sampling oscilloscope (Agilent 86100A) and the spectra are measured by an

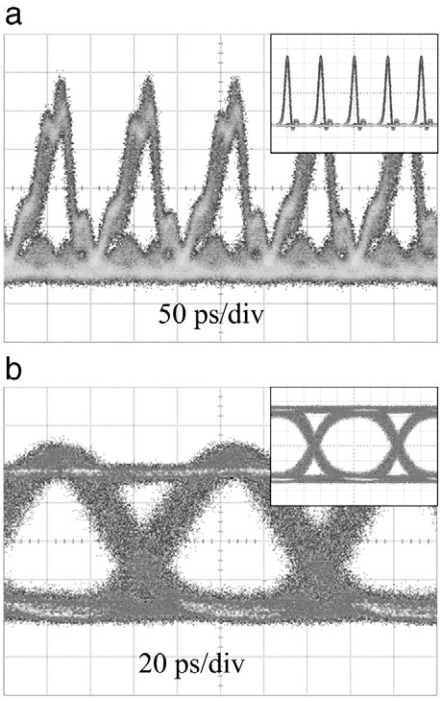

Fig. 2. Eye diagrams of the 10-Gb/s degraded (a) RZ signal and (b) NRZ signal injected to the proposed clock recovery scheme. Inset: the original signals.

electrical spectrum analyzer (ESA, Agilent 8593E). In addition, an optical spectrum analyzer (OSA: Ando AQ 6315B) with a resolution of 0.05 nm is employed to monitor the optical spectra.

To demonstrate the feasibility of the clock recovery, a 9.953-Gb/s optical RZ signal at 1547.8 nm is generated. A dynamically-varied differential group delay element with a maximum differential group delay of 32 ps followed by a dispersive element with a dispersion parameter of −96 ps/nm, which simulates long-haul fiber with residual PMD of 32 ps and residual dispersion of 96 ps/nm, is used to degrade the signal. The eye diagram of the RZ signal is shown in Fig. 2(a). As compared with the original signal shown in the inset of Fig. 2(a), the degraded signal has serious inter-symbol interference and large timing and amplitude jitters. Fig. 3 shows the experiment results of the clock recovery from the degraded RZ signal. As can be seen from Fig. 3(a), stable electrical clock is obtained at the electrical output port of the OEO. The large timing jitter in the degraded signal is significantly reduced since the OEO is a high-Q oscillator. Fig. 3(b) depicts the electrical spectrum of the recovered clock. The clock is centered at 9.953 GHz with an extinction ratio of more than 51 dB measured by the ESA with a resolution bandwidth of 3 kHz. From Fig. 3(b), we can estimate that the timing jitter of the recovered clock is 150 fs [7]. To demonstrate that the clock is extracted from the input data signal, the electrical clock is served as a trigger for the sampling oscilloscope. The eye diagram is shown in Fig. 3(c), which is almost the same as that in Fig. 2(a), indicating that the injected data signal is well synchronized to the recovered clock. High-quality dual-wavelength optical clocks are achieved at the optical output port. As shown in Fig. 3(d), the wavelength spacing is 2.38 nm, which agrees well with the theory in [13].The frequency combs with a 0.08-nm spacing are clearly seen, indicating the short-time stability of the scheme is excellent. The bandwidths of the two wavelengths are 0.18 and 0.17 nm. We confirm the existence of pulses at the two wavelengths by inserting a tunable OBPF with a 3-dB bandwidth of 0.6 nm external to the optical output port. The obtained waveforms at the two wavelengths are shown in the insets of Fig. 3(d). The pulse widths estimated by the oscilloscope are 34.3 and 33.3 ps. The time bandwidth products are calculated to be 0.772 and 0.708. For Gaussian pulse shape, the pulses are chirped. In the experiment, the PRBS length is switched from 2^7-1 to $2^{31}-1$, no evident changes on the waveforms are observed, demonstrating that the pattern effect does not occur in the scheme.

By adjusting the cavity length of the MLFRL and changing the center frequency of OBPF2, the wavelengths of the recovered optical clock can be tuned from 1528.5 to 1567.2 nm except for a region close

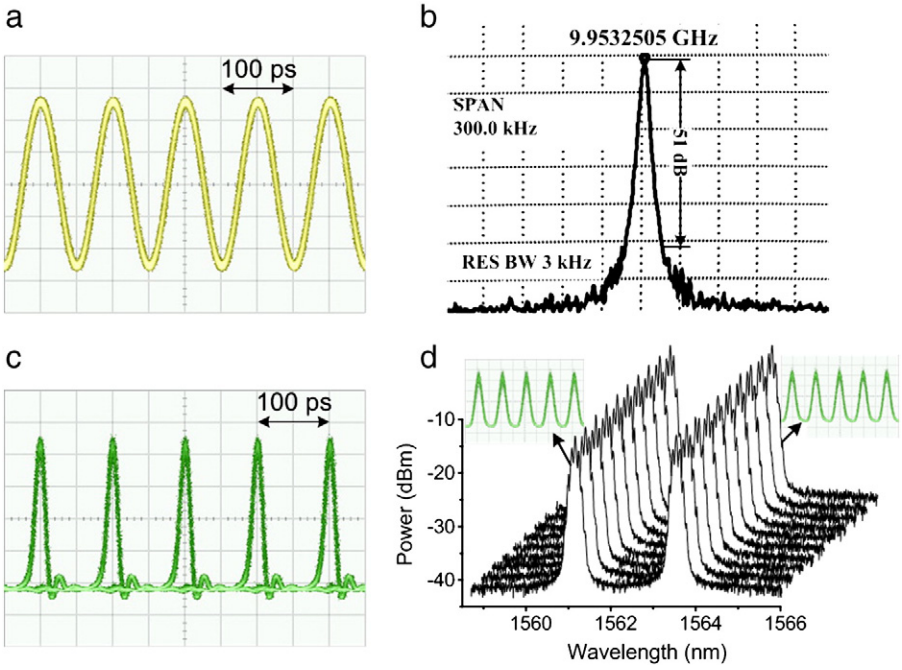

Fig. 3. (a) The waveform of the recovered electrical clock from the degraded RZ signal; (b) the electrical spectrum of the recovered clock; (c)waveform of the 10 Gb/s original RZ signal triggered by the OEO oscillating signal; (d) the repeated scan of the optical spectra at the optical clock output port with a time interval of 5 min.

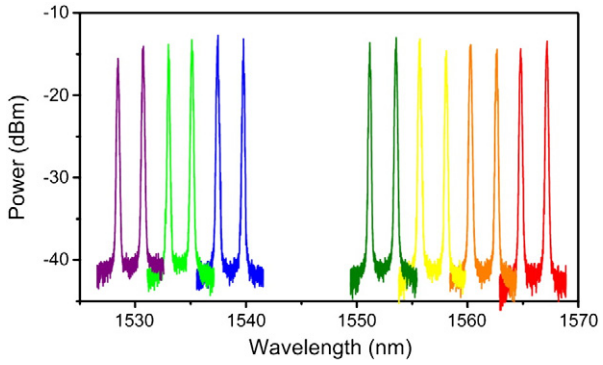

Fig. 4. Optical spectra when the two wavelengths are tuned from 1528.5 to 1567.2 nm.

to the wavelength of the injected data signal, i.e. 1547.8 nm, as shown in Fig. 4. The pulse widths of the obtained clocks are from 29 to 38 ps, and the spectral widths are from 0.17 to 0.20 nm.

The injection locking status is maintained when the RZ signal is replaced by a degraded NRZ signal. In this case, the 9.953-Gb/s optical NRZ signal is degraded by a section of 24-km single-mode fiber (SMF). The eye diagrams of the degraded and original signals are shown in Fig. 2 (b), and the results of clock recovery are shown in Fig. 5. For the recovered electrical clock, the power is reduced by 5 dB and the timing jitter is increased to 170 fs. This is because the clock components in the NRZ signal is very weak. For the optical clock, the dual-wavelength operation is still obtained. Wavelength tuning of the optical clock from 1530 to 1565 nm is also verified by adjusting the cavity length of the MLFRL and changing the center frequency of OBPF2.

4. Discussion

For practical implementing the clock recovery, it would be very important to understand the stability of the proposed scheme. Since an OEO would have a certain tracking and locking range [7], it can tolerate environment variation to some extent, which ensures the stability of the electrical clock. However, the loop of MLFRL has a long fiber, so the operation should be sensitive to the environment changes. To evaluate the stability, the scheme is allowed to be operated in a room environment for a period of 60-min. The optical spectra of the generated dual-wavelength optical clock are recorded in the OSA with a time interval of 5 min. As shown in Fig. 3(d) and Fig. 5(b), the wavelength shift is larger than 0.2 nm and the optical power fluctuation is greater than 0.5 dB. But it is interesting to find that the waveforms of the recovered clock are almost unchanged, indicating the mode-locking state is maintained. This situation can be explained as follows. Assume that the MLFRL firstly operates at the steady state. Then the cavity length is changed, so the mode-locking condition is broken and the laser is working at the detuning state, in which the pulse is distorted and its peak deviates from its original position in the time domain. The distortion of the pulse results in a spectral change. Thus, the spectral peak shifts to another wavelength. The wavelength shift compensates for part the detuning of the laser thanks to the large dispersion in the cavity. This process repeats several times until new steady state is established. The pulse peak returns to its original position in the time domain. Meanwhile, the wavelength is changed. It should be noted that if the mode-locking state of MLFRL is not affected by the environment variation, it would be very easy to apply a feedback loop to compensate the change of the cavity length and to guarantee the long term stability of the scheme.

The proposed scheme can be altered to perform clock extraction from higher data-rate signals. The upper bound of the operational frequency is limited by the bandwidth of the key devices in the OEO loop, such as the MZM, EA and PD. Since 40-GHz MZM, EA and PD are already available, the method can be applied in 40 Gb/s systems. Furthermore, if a frequency doubling OEO [8] is used to replace the conventional OEO, the scheme may be available for 80 Gb/s systems.

In addition, according to [16], optical clocks at more wavelengths are possible by optimizing the dispersion value of the two dispersive elements and the 3-dB bandwidth of OBPF2.

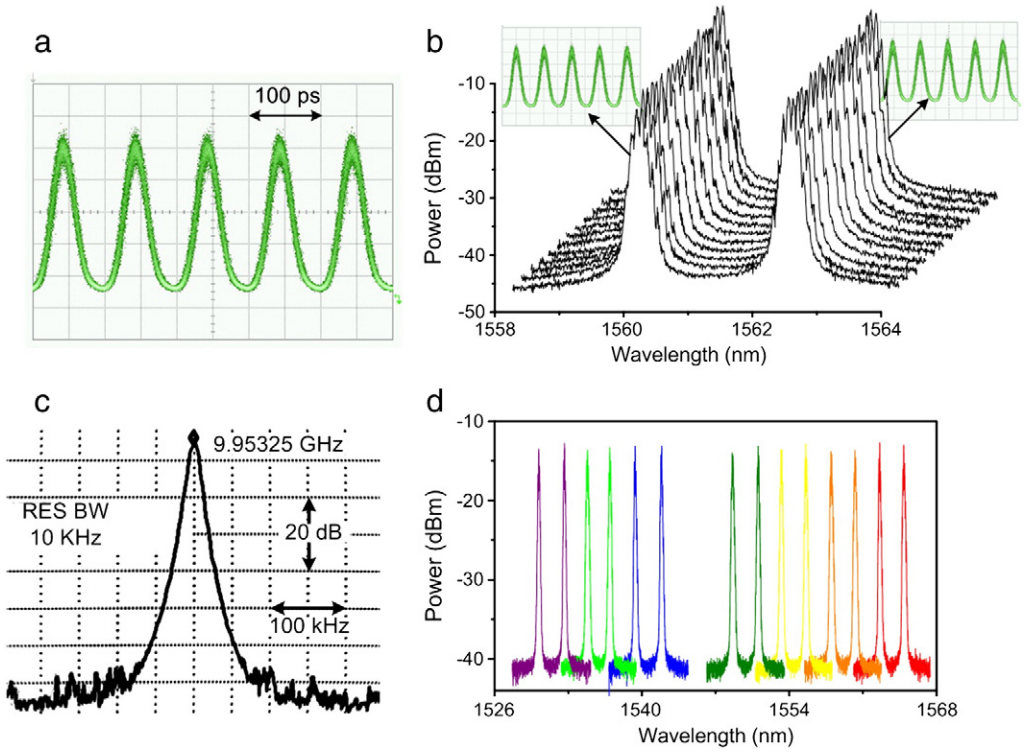

Fig. 5. (a) The waveform of the recovered optical clocks at two wavelengths from the degraded NRZ signal; (b) the repeated scan of the optical spectra at the optical clock output port with a time interval of 5 min; (c) the electrical spectrum of the recovered clock; (d) optical spectra when the two wavelengths are tuned from 1530.2 to 1565.0 nm.

5. Conclusion

An optical clock recovery scheme composed of an OEO and a dual-wavelength MLFRL with a distributed dispersion cavity was proposed and demonstrated. Dual-wavelength 10-GHz optical clocks with a timing jitter less than 170 fs and wavelengths tunable from 1530 to 1565 nm were experimentally recovered from 10-Gb/s degraded RZ and NRZ signals.

Compared with the previously reported approaches [3,5–9], the proposed technique has two major advantages: 1) the system can obtain simultaneously dual- or multi-wavelength synchronized clocks for composite optical signal processing; 2) the system can operate in either RZ or NRZ system using the same configuration. In addition, the system is free of pattern effects and can tolerate certain signal degradation, which may find applications in future optical signal processing subsystems.

Acknowledgement

This work was supported in part by the “973” Major State Basic Research Development Program of China under grant 20llCB301703 and the Program for New Century Excellent Talents in University (NCET).

References

[1] T. von Lerber, S. Honkanen, A. Tervonen, H. Ludvigsen, F. Kppers, Opt. Fiber Technol. 15 (2009) 363.
[2] K. Smith, J.K. Lucek, Electron. Lett. 28 (1992) 1814.
[3] T. Ohno, K. Sato, R. Iga, Y. Kondo, I. Ito, T. Furuta, K. Yoshino, H. Ito, Electron. Lett. 40 (2004) 265.
[4] Y. Yu, X.L. Zhang, D.X. Huang, IEEE Photon. Technol. Lett. 18 (2006) 2356.
[5] P.E. Barnsley, H.J. Wickes, G.E. Wickens, D.M. Spirit, IEEE Photon. Technol. Lett. 3 (1991) 942.
[6] H. Dong, H.Z. Sun, G.H. Zhu, Q. Wang, N.K. Dutta, Opt. Express 12 (2004) 4751.
[7] L. Huo, Y. Dong, C.Y. Lou, Y.Z. Gao, IEEE Photon. Technol. Lett. 15 (2003) 981.
[8] S.L. Pan, J.P. Yao, J. Lightwave Technol. 27 (2009) 3531.
[9] Z.X. Wang, T. Wang, C.Y. Lou, L. Huo, Y.Z. Gao, Opt. Commun. 219 (2003) 301.
[10] G.K.P. Lei, C. Shu, M.P. Fok, IEEE Photon. Technol. Lett. 22 (2010) 571.
[11] H. Hu, J.L. Yu, L.T. Zhang, A.X. Zhang, W.R. Wang, J. Wang, Y. Jiang, E.Z. Yang, IEEE Photon. Technol. Lett. 20 (2008) 1181.
[12] W.Z. Li, H.M. Zhang, Q.W. Wu, Z.Q. Zhang, M.Y. Yao, IEEE Photon. Technol. Lett. 19 (2007) 625.
[13] S.L. Pan, X.F. Zhao, W.K. Yu, C.Y. Lou, Opt. Laser Technol. 40 (2008) 854.
[14] C. O'Riordan, M.J. Connelly, Opt. Commun. 283 (2010) 1865.
[15] P. Myslinski, C. Barnard, G. Cheney, J. Chrostowski, B. Syrett, J. Glinski, Opt. Commun. 97 (1993) 340.
[16] S.L. Pan, C.Y. Lou, IEEE Photon. Technol. Lett. 18 (2006) 604.
[17] S.L. Pan, J.P. Yao, IEEE J. Sel. Top. Quantum Electron. 16 (2010) 1460.
[18] S. Fu, M. Tang, W.-D. Zhong, Y.J. Wen, P. Shum, IEEE Photon. Technol. Lett. 19 (2007) 925.
[19] H.K. Lee, J.T. Ahn, M. Jeon, K.H. Kim, D.S. Lim, C. Lee, IEEE Photon. Technol. Lett. 11 (1999) 730.